Title

Knudsen cell studies of the reactions of N2O5 and ClONO2 with NaCl: development and application of a model for estimating available surface areas and corrected uptake coefficients

Journal

Physical Chemistry Chemical Physics, 5(9)

ISSN

14639076 14639084

Authors

Hoffman, Rachel C
Gebel, Michael E
Fox, Brigitte S
et al.

Publication Date

2003-04-16

DOI

10.1039/b301126g

Peer reviewed

PCCP

Knudsen cell studies of the reactions of N_2O_5 and $ClONO_2$ with NaCl: development and application of a model for estimating available surface areas and corrected uptake coefficients

Rachel C. Hoffman, Michael E. Gebel,† Brigitte S. Fox‡ and Barbara J. Finlayson-Pitts*

Department of Chemistry, University of California, Irvine, CA 92697-2025. E-mail: bjfinlay@uci.edu; Fax: +1 (949) 824-3168; Tel: +1 (949) 824-7670

Received 28th January 2003, Accepted 27th February 2003
First published as an Advance Article on the web 21st March 2003

The reaction of gaseous N_2O_5 with sea salt and its components is a potential source of halogen atoms in the marine boundary layer. There are two possible reaction paths when water is present on the salt surface. Reaction with the chloride ion forms nitryl chloride ($ClNO_2$), a photolyzable compound: $N_2O_5 + NaCl \rightarrow ClNO_2 + NaNO_3$, while hydrolysis of N_2O_5 generates HNO_3 that can react further with NaCl to form gaseous HCl: $N_2O_5 + H_2O$ (on NaCl) $\rightarrow 2\ HNO_3$, $HNO_3 + NaCl \rightarrow HCl + NaNO_3$. We report here Knudsen cell studies at 23 °C of the reaction of N_2O_5 with NaCl, using less than one layer of salt particles. A model, which takes into account the effective salt surface area exposed to the gas, was applied, allowing for the determination of uptake coefficients without introducing uncertainties associated with diffusion into multiple layers of salt particles. The net uptake coefficient for the sum of both channels for the N_2O_5 reaction was measured to be $\gamma_{N_2O_5} = (2.9 \pm 1.7) \times 10^{-3}$, where the error cited is the 2σ statistical error. The cumulative error is estimated to be better than a factor of three. Both $ClNO_2$ and HCl were observed as gaseous products from the N_2O_5-salt reaction and the branching ratio for $ClNO_2$ was 0.73 ± 0.28 (2σ). A limited number of experiments were carried out for the reaction with synthetic sea salt, resulting in an uptake coefficient of about an order of magnitude larger than for NaCl, and a $ClNO_2$ yield of 100%. We propose a mechanism for this reaction in which surface-adsorbed water plays a key role in the competition between hydrolysis of N_2O_5 to generate HNO_3 and the reaction with NaCl to generate $ClNO_2$. Reaction with NaCl is shown to be a potentially important source of $ClNO_2$, and thus, of highly reactive chlorine atoms in urban marine regions at dawn. Application of our model to previous data from this laboratory for the reaction of chlorine nitrate ($ClONO_2$) with fractional layers of NaCl gives a corrected uptake coefficient of $\gamma_{ClONO_2} = (2.4 \pm 1.2) \times 10^{-2}$ (2σ), which suggests that the $ClONO_2$–NaCl reaction may contribute significantly to the observed concentrations of Cl_2 in the marine boundary layer.

I. Introduction

A major source of nitric acid (HNO_3) in the atmosphere is the hydrolysis of N_2O_5 on particles and other surfaces that hold water:[1–9]

$$N_2O_5 + H_2O \rightarrow 2\ HNO_3 \quad (1)$$

This hydrolysis is believed to occur through the autoionization of N_2O_5 in solution and/or at the aqueous surface, followed by the reaction of NO_2^+ with water to produce HNO_3. However, if chloride ions are present, there is a competition between the reactions of NO_2^+ with water and Cl^-, and $ClNO_2$ is generated:[3,5,8,10–16]

$$N_2O_5 + NaCl \rightarrow NaNO_3 + ClNO_2 \quad (2)$$

As a result, the reaction of N_2O_5 with deliquesced NaCl or sea salt, with aqueous solutions of NaCl, or with solid NaCl that holds surface-adsorbed water (SAW)[17–22] could potentially proceed by two paths, one generating HNO_3 and one generating $ClNO_2$. In the former case, the HNO_3 product can react further with NaCl[11–18,20,22–34] to generate HCl. Hydrochloric acid is photochemically inert in the lower troposphere, reacts relatively slowly with OH radicals, and is removed in large part in the boundary layer by wet and dry deposition. In contrast, $ClNO_2$ can be readily photolyzed during the daytime producing chlorine atoms. Such highly reactive atomic chlorine in the troposphere has the potential to impact the oxidative balance and overall atmospheric chemistry in the marine boundary layer.[35–45]

In order to assess the importance of chlorine atoms, it is important to elucidate the kinetics, products, and mechanisms for reaction of N_2O_5 with sea salt and its major component, NaCl. The reaction of N_2O_5 with solid NaCl, suspended aerosol particles, and aqueous solutions of NaCl has been studied using a number of different analytical techniques. These studies are summarized in Table 1. The reaction of N_2O_5 with deliquesced aerosol particles or aqueous solutions of NaCl is fast, with uptake coefficients in the range of $(1–5) \times 10^{-2}$, similar to that for N_2O_5 uptake on water.[1–9] The reported uptake coefficients for the reaction with solid NaCl are less consistent, ranging from less than 10^{-4} to greater than 2.5×10^{-3}. The yield of $ClNO_2$ (and hence, the branching ratio between $ClNO_2$ and HNO_3/HCl) is quite variable in the studies of the solids and the aerosol particles, ranging from 31 to 100%.

A common difficulty in measuring uptake coefficients is that multiple layers of salt crystals, into which the gaseous reactant can diffuse, are often used. This introduces substantial uncertainty regarding the available surface area of the salt to which

† Current address: Monitoring and Laboratory Division, California Air Resources Board, 9528 Telstar Ave., El Monte, CA 91731, USA.
‡ Current address: Institut für Physikalische und Theoretische Chemie, Technische Universitaet München, Lichtenbergstr. 4, 85747 Garching, Germany

 DOI: 10.1039/b301126g

Table 1 Summary of previous work on the uptake and reaction of N_2O_5 on solid and aqueous NaCl.[a]

NaCl phase	Analytical technique	Researchers	Uptake coefficient (γ)	Yield of $ClNO_2$ (%)
Solid	FTIR	Livingston and Finlayson-Pitts, 1991[10]	$> 2.5 \times 10^{-3}$	60–100
	Annular reactor	Msibi *et al.*, 1994[11]	1×10^{-3}	nd[b]
	Flow tube/EI MS[b]	Leu *et al.*, 1995[12]	$<10^{-4}$ for dry salts; $\sim 4.5 \times 10^{-4}$ for slightly wet salts	nd[b]
	Knudsen Cell/MS	Fenter *et al.*, 1996[13]	$(0.9–2.0) \times 10^{-3}$ for powders [c]	60
	Diffusion tube/MS	Koch *et al.*, 1999[14]	$(3 \pm 1) \times 10^{-4}$	100
Aerosol particles	Chamber/IC	Behnke *et al.*, 1991;[15] Zetzsch *et al.*, 1992[16]	$(2.4–5.0) \times 10^{-2}$ [d]	61–31 [e]
	Droplet train/FTIR[f]	George *et al.*, 1994[3]	$(1.4–3.9) \times 10^{-2}$ [f]	nd[b]
	Chamber/FTIR	Behnke *et al.*, 1997[5]	$(3.2 \pm 0.2) \times 10^{-2}$ [g]	65
	Droplet train/FTIR and MS	Schweitzer *et al.*, 1998[8]	1.5×10^{-2} [f]	100 ± 14
Solution	Annular reactor	Msibi *et al.*, 1994[11]	$\sim 1.5 \times 10^{-2}$	nd[b]
	Wetted wall flow tube/FTIR[h]	Behnke *et al.*, 1997[5]	nd[b]	95 [h]

[a] At room temperature, unless otherwise noted. [b] nd = not determined [c] For spray-coated NaCl, and polished and depolished window faces, the uptake coefficients were smaller, from $(<0.1–0.5) \times 10^{-3}$. [d] Over a RH range of 71 to 92%. [e] Highest yield for lowest % RH where droplets are more concentrated. [f] Over a temperature range of 262–278 K [g] For concentrations of NaCl in solution $\geq$ 1 M and RH between 77.3 and 93.9%. [h] For a 5M NaCl concentration in which the $ClNO_2$ yield had peaked.

the gas is exposed.[12,13,17,32,46–52] In the limit of very fast gas uptake, the gas is removed before it can diffuse significantly into the underlying salt layers. In this case, the geometric surface area is a reasonable approximation for the available reactive surface area. In the other extreme of a very slow reaction, diffusion throughout the salt layers can occur and the reactive surface area encompasses the entire salt sample. However, in the intermediate regime, a correction must be made for the extent of diffusion of the gas into the salt layers. Diffusion followed by reaction of gases in multiple salt layers may also potentially affect measured yields of gas phase products, since they can undergo secondary reactions during transport to the top of the salt layers. Some models have been developed to correct the measured uptake coefficients for diffusion into the underlying layers,[46,47] but it would be valuable to carry out measurements under conditions for which uncertainties due to such corrections are not present.

To address these issues, we have conducted studies of the uptake of N_2O_5 on solid NaCl, representative of the major component of sea salt aerosol, using a Knudsen cell with less than one layer of salt. A model is presented that takes into account not only the top surfaces of the salt particles but also the fraction of particle sides that are available for reaction due to the scattering of the reactant gas from the sample holder. The gaseous products, $ClNO_2$ and HCl, were measured in order to probe the relative importance of reactions (1) and (2). The uptake of N_2O_5 on synthetic sea salt (SSS) powders, for which there are no literature data, was also studied in a limited number of experiments. Finally, this model for the gas reaction with less than one layer of salt is applied to data previously obtained[21] for the reaction of $ClONO_2$ with fractional layers of NaCl, a reaction that generates molecular chlorine:

$$ClONO_2 + NaCl \rightarrow Cl_2 + NaNO_3 \qquad (3)$$

It is shown that the reactions of N_2O_5 and $ClONO_2$ with NaCl may contribute to the chemistry of coastal urban areas where there are substantial sources of oxides of nitrogen to form N_2O_5 and $ClONO_2$.

II. Experimental methods

Experiments were performed at room temperature using a glass Knudsen cell equipped with a moveable lid for covering the sample, described in detail elsewhere.[17,21,26] Reactant gases were introduced into the cell from a glass gas-handling manifold through a stainless steel needle valve coated with halocarbon wax (Halocarbon Products, Series 1500). Salt powders were contained in a halocarbon wax-coated stainless steel holder with a diameter of 4.9 cm. The pressure was monitored using a BOC Edwards (Model 655AB) absolute pressure sensor (0–50 mTorr) equipped with an Edwards readout unit (Model AGC No. R232). The pressure within the cell was $\leq$0.3 mTorr, sufficiently low to ensure that experiments were conducted in the molecular flow regime. The Knudsen cell was interfaced to a quadrupole mass spectrometer with an electron impact ionizer (ABB Extrel, EMBA II 150-QC) through one of two removable glass apertures with hole diameters of 3.9 and 5.8 mm, chosen to optimize the uptake signal. Ion current signals were obtained by phase sensitive detection and processed with a lock-in amplifier (EG&G, Model 5209) interfaced to a computer with data acquisition software (ABB Extrel, Merlin, Rev. B).

Salt samples were obtained commercially. NaCl single crystals were obtained from Reflex or Bicron, NaCl powders from Fluka, and SSS from Aquarium Systems (Instant Ocean®) (the composition of SSS is discussed in ref. 53). NaCl salt samples were prepared to yield different average particle sizes. A few experiments were carried out initially to probe for diffusion effects using multiple layers of finely ground salts, obtained by mechanical grinding using a Wig-L-Bug® amalgamator (Crescent Dental, Model 3110-3A) for five minutes. Scanning electron microscopy (SEM) images showed these salts to have a wide distribution of sizes with an average of about 10 μm. For the experiments using less than a single layer of salt, samples were obtained by sieving (U.S. Standard sieve #40) either commercially available powders or crushed cuttings to obtain the desired size. For the commercially available powders, the average particle size was found to be 312 μm and the particles were cubic in shape.[29] The average size of particles obtained from crushed and similarly sieved single crystal cuttings was determined from SEM images[29] to be 428 μm. The larger average size for the crushed single crystal samples is due to the irregular shapes produced in the grinding process. Ghosal and Hemminger[22] have shown that the most finely ground powders hold significant amounts of water even under vacuum, while 500 μm particles were shown to hold less but still measurable

amounts. Water was undetectable on the surface of single crystal NaCl (100).

SSS was similarly crushed and sieved to give an average coarse particle size of about 400 μm. It is known that SSS contains substantial amounts of water, for example, in the form of $MgCl_2 \cdot 6H_2O$; in addition, such components also help to physisorb additional amounts of water on the salt surface.[26,53]

N_2O_5 was synthesized by the reaction of NO_2 with excess O_3. A stream of ~5 % O_3 in O_2, dried using P_2O_5, was passed over condensed NO_2 and the products collected in a trap using an ethanol/liquid N_2 slush bath held at −70 °C by varying the ratio of ethanol to liquid N_2. After the reaction was complete, unreacted NO_2 was removed by pumping on the trap while holding it at ~ −50 °C. Hydrolysis of N_2O_5 also occurs on surfaces of the traps, generating HNO_3 as an impurity ranging from 8 to 39 %. The amount of HNO_3 impurity was determined by FTIR using a 10 cm glass cell and the published cross sections from Wangberg *et al.*[54] of 9.29×10^{-19} and 8.56×10^{-19} cm^2 $molecule^{-1}$ for HNO_3 and N_2O_5, respectively. The uncertainty in the determination of the HNO_3 impurity was ±8 % (2σ) based on repeated measurements of the same N_2O_5 mixture. However, there is a large uncertainty associated with the fact that during measurement of the impurity in the FTIR cell, the N_2O_5 is exposed to a system with a larger surface to volume ratio than in the Knudsen cell experiments; this will enhance the formation of HNO_3 from the surface hydrolysis of N_2O_5. In addition, the surface of the FTIR cell is borosilicate glass, which has been shown by experiments conducted in this laboratory to be much more reactive toward N_2O_5 hydrolysis than the halocarbon-wax coated surface of the Knudsen cell. We therefore believe the impurity measured in the FTIR cell to represent an upper limit of the HNO_3 impurity present in the Knudsen cell experiments. The impact of this uncertainty on the results is treated quantitatively below (Section III.C).

Nitryl chloride was synthesized from the reaction of HCl with excess N_2O_5. N_2O_5 was condensed in a conditioned glass trap at ~−70 °C using an ethanol/liquid N_2 slush bath, and HCl subsequently added to the trap. The reaction trap was first allowed to warm to room temperature to maximize the extent of reaction and then cooled with liquid nitrogen. Subsequently, the mixture was brought to −70 °C again and pumped on briefly to remove Cl_2. Small amounts of impurity nitrosyl chloride were removed by reacting the mixture with O_3 to form $ClNO_2$. At this point, pure $ClNO_2$ was drawn off the cold trap and examined using FTIR to ensure there were no detectable impurities present.

Dry HNO_3 gas was obtained from the vapor over a solution of concentrated HNO_3 and H_2SO_4 (1 : 2 v/v). Concentrated HNO_3 (Fisher, 69.7 wt. %), concentrated H_2SO_4 (Fisher, 96.0 wt. %), HCl gas (Scott Specialty Gases, 99.995%), NO (Matheson, High Purity, 99.5%), and O_2 (Oxygen Service Co., Ultrahigh Purity) were used without further purification.

A. Uptake coefficient determination. In the Knudsen cell, reactant gas molecules either exit through an aperture into the mass spectrometer or are lost by uptake on the reactive surface. A net uptake coefficient for N_2O_5, $\gamma_{N_2O_5}$, can be determined from the relative loss on the surface to that through the exit aperture:[13,45,55,56]

$$\gamma_{N_2O_5} = \left(\frac{I_0}{I_r} - 1\right)\left(\frac{A_{aperture}}{A_{surface}}\right) = \left(\frac{[N_2O_5]_0}{[N_2O_5]_r} - 1\right)\left(\frac{A_{aperture}}{A_{surface}}\right) \quad (I)$$

Here, I_0 and I_r are the steady-state reactant signals with the surface covered and when the reactive surface is exposed, respectively, and are proportional to $[N_2O_5]_0$ and $[N_2O_5]_r$. $A_{aperture}$ is the area of the exit aperture and $A_{surface}$ is the area of the reactive salt surface. In the initial data analysis, $\gamma_{N_2O_5}$ was calculated using the geometric surface area of the sample holder for $A_{surface}$, denoted $\gamma_{N_2O_5}^{geometric}$. To estimate the true available surface area using less than one layer of particles, a model was developed that is described in detail below. This model incorporates both the tops of the particles as well as a fraction of the particle sides.

The mass spectra of the species of interest in this study share common fragment peaks when using electron impact ionization (Fig. 1). N_2O_5 does not have a measurable parent peak under our experimental conditions; the most intense peak is its fragment at $m/z = 46$. However, the HNO_3 impurity also contributes to the $m/z = 46$ signal, as does the $ClNO_2$ product once the lid is opened exposing the salt. To correct for these contributions and obtain $[N_2O_5]_0$ and $[N_2O_5]_r$ in eqn. (I), the following approach was taken. (1) While the salt was covered,

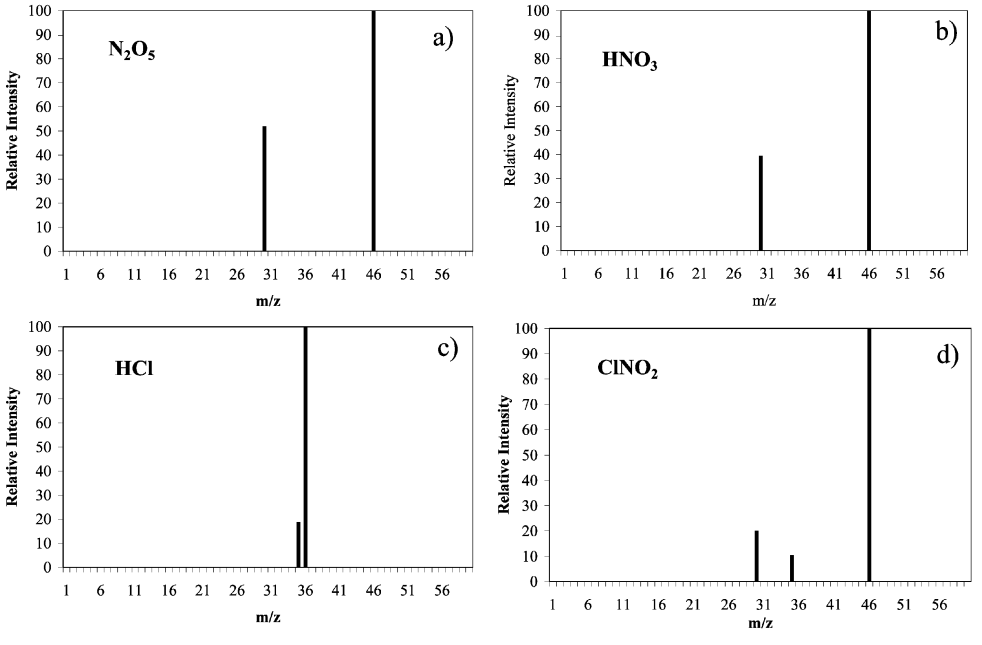

Fig. 1 Mass spectral relative peak intensities measured using electron impact ionization for (a) N_2O_5, (b) HNO_3, (c) HCl, and (d) $ClNO_2$.

and hence not reacting with N_2O_5, the $m/z = 46$ signal was corrected for the contribution from the impurity HNO_3 ($I_0^{HNO_3}$) calculated based on the FTIR measurements of the HNO_3 impurity and the mass spectrometer calibration for HNO_3 in the Knudsen cell. (2) The remaining $m/z = 46$ signal while the salt was covered was assigned to N_2O_5 ($I_0^{N_2O_5}$) : $I_0^{N_2O_5} = I_0 - I_0^{HNO_3}$. The N_2O_5 concentration, $[N_2O_5]_0$, corresponding to this signal was calculated from a mass spectrometer calibration for N_2O_5 (corrected for the HNO_3 impurity). Even at the highest % HNO_3 impurity, 75% of the signal at $m/z = 46$ is attributable to N_2O_5 when the lid is closed.

When the lid is lifted to expose the salt, N_2O_5 is taken up and reacts on the salt surface, resulting in a decrease in the N_2O_5 concentration, $[N_2O_5]_r$, and signal, I_r. To determine $[N_2O_5]_r$, it was recognized that, when the lid is lifted, both reaction (2) of N_2O_5 with NaCl and the hydrolysis (4) of N_2O_5 with water on the salt surface occur:

$$N_2O_{5\,(g)} + H_2O/NaCl \rightarrow 2\ HNO_{3\,(surface)} \rightarrow 2\ HCl_{(g)}^{hydrolysis} \quad (4)$$

Based on previous studies of the gaseous products of the HNO_3–NaCl reaction,[12,13,17,18,29,32] HNO_3 generated in the N_2O_5 hydrolysis reacts on the salt surface to form gaseous HCl. We denote the HCl produced in reaction (4) as $HCl^{hydrolysis}$. For each N_2O_5 reacted in reaction (2), one $ClNO_2$ is formed and for each N_2O_5 undergoing hydrolysis (4) on the surface, two HCl molecules are formed. Therefore, from mass balance, the amount of unreacted N_2O_5 remaining in the cell upon reaction, $[N_2O_5]_r$, must be given by:

$$[N_2O_5]_r = [N_2O_5]_0 - [ClNO_2] - \tfrac{1}{2}[HCl]^{hydrolysis} \quad (II)$$

The concentration of $ClNO_2$ was obtained by the following analysis. As seen in Fig. 1, $ClNO_2$ has peaks at $m/z = 30$, 35, and 46, while HCl has a peak at $m/z = 35$ and 36. The peak at $m/z = 36$ is unique to HCl, while that at $m/z = 35$ is due to a combination of HCl and $ClNO_2$. Therefore, the concentration of HCl was calculated from the unique peak at $m/z = 36$ and the mass calibration for this gas. The portion of the signal at $m/z = 35$ due to HCl was quantified using the HCl mass spectral calibration in the Knudsen cell, and the excess measured signal at $m/z = 35$ above that due to HCl was then assigned to $ClNO_2$. The concentration of $ClNO_2$, $[ClNO_2]$, was then calculated from this excess $m/z = 35$ signal and a calibration using a synthesized sample of pure $ClNO_2$.

The final step in determining $[N_2O_5]_r$ in eqn. (II) is to compute the concentration of HCl generated by the hydrolysis of N_2O_5 on the salt surface, $[HCl]^{hydrolysis}$. The total concentration of HCl during the experiment was measured as described above using its unique peak at $m/z = 36$. This total HCl, $[HCl]^{measured}$, is due to a combination of that produced from the reaction of the HNO_3 impurity initially present in the N_2O_5 reactant gas, $[HCl]^{impurity}$, and that from the N_2O_5 hydrolysis reaction (4) on the salt surface, $[HCl]^{hydrolysis}$:

$$[HCl]^{measured} = [HCl]^{impurity} + [HCl]^{hydrolysis} \quad (III)$$

The value of $[HCl]^{impurity}$ was calculated based on the uptake coefficient of HNO_3 on NaCl (γ_{HNO_3}) under the same experimental conditions, determined in a separate study.[29] Eqn. (IV) was applied to determine the reduction in the HNO_3 impurity signal at $m/z = 46$ ($I_r^{HNO_3}$) due to the direct reaction of impurity HNO_3 with NaCl:

$$I_r^{HNO_3} = \frac{I_0^{HNO_3}}{\gamma_{HNO_3}\dfrac{A_{surface}}{A_{aperture}} + 1} \quad (IV)$$

where $I_0^{HNO_3}$ is the signal of the HNO_3 impurity initially in the N_2O_5 mixture. This calculated signal ($I_r^{HNO_3}$) was then converted to the unreacted impurity concentration of HNO_3 with the lid open using a mass spectrometer calibration. The difference between the initial impurity HNO_3 and that calculated using eqn. (IV) is the amount of the impurity HNO_3 that has reacted. Since one impurity HNO_3 molecule generates one HCl molecule, the concentration of HCl generated, $[HCl]^{impurity}$, can be calculated. Using the mass balance eqn. (III), $[HCl]^{hydrolysis}$ is then obtained. Finally, $[N_2O_5]_r$ is calculated using eqn. (II) and the uptake coefficient, $\gamma_{N_2O_5}$, is obtained from eqn. (I).

This analysis takes into account the fact that the signal at $m/z = 46$ when the lid is open has contributions from unreacted N_2O_5, product $ClNO_2$, and the impurity HNO_3 that has not reacted. In the case of the highest percentage of HNO_3 impurity, the contributions of HNO_3 to the $m/z = 46$ signal is approximately 24%, that due to $ClNO_2$ is approximately 13% and the remainder is due to unreacted N_2O_5. The potential error in $\gamma_{N_2O_5}$ in a typical experiment due to these corrections is discussed below (Section III.C).

Additionally, to assess the extent that reaction with NaCl *versus* hydrolysis contributes to the uptake and reaction of N_2O_5, the branching ratio for $ClNO_2$, BR^{ClNO_2}, *i.e.* the fraction of the net uptake of N_2O_5 that forms $ClNO_2$, was calculated from eqn. (V):

$$BR^{ClNO_2} = \left(\frac{[ClNO_2]}{[ClNO_2] + \frac{1}{2}[HCl]^{hydrolysis}}\right) \quad (V)$$

III. Results

A. Uptake of N_2O_5 on NaCl powders. To carry out an initial assessment of the dependence of the uptake on the number of salt layers, a few studies were carried out using multiple layers of finely ground salts prepared in a similar manner to those used in earlier Knudsen cell studies of the HNO_3 and $ClONO_2$ reactions.[17,21] Fig. 2 shows the results of a typical experiment using multiple layers of NaCl powder. Upon exposure of the salt, there is a sharp drop in the $m/z = 46$ signal with an accompanying increase in the $m/z = 36$ and 35 signals. The ratio of the $m/z = 36$ to 35 signals in Fig. 2 at 250 seconds is 73% of that for a pure sample of HCl under the same conditions. The smaller ratio than expected from HCl alone indicates that there is an additional contribution to the signal at $m/z = 35$, *i.e.* that $ClNO_2$ is also being produced. Using eqn. (V), the branching ratio for $ClNO_2$ was calculated to be 0.81 for this experiment.

The slower recovery of the $m/z = 36$ signal compared to the 46 signal upon closing the lid is likely due to desorption of HCl from the halocarbon-wax coated cell walls. As seen at t = 0, there is some HCl which is due to displacement of HCl from the walls by HNO_3. The smaller gas phase HNO_3 concentration when the lid is opened allows additional HCl to be taken up on the cell walls which then desorbs when the lid is closed and the HNO_3 concentration returns to its previous level. Uptake coefficients were determined using steady-state signals, not these regions of decline, and hence this has no impact on the results reported here.

Fig. 3 summarizes the uncorrected uptake coefficients for N_2O_5, *i.e.* those measured assuming the available reactive surface area is the geometric area of the sample holder ($\gamma_{N_2O_5}^{geometric}$), as a function of the number of salt layers for these multi-layer samples. It is seen that these uncorrected uptake coefficients are of the order of 10^{-3}, in the mid-range of values where some diffusion into the underlying salt layers is expected to be important. Consistent with this, the uncorrected uptake coefficient increases with the number of particle layers. These observations show conclusively that diffusion into the bulk sample is important and that the measured values must therefore be corrected for the true available surface area.

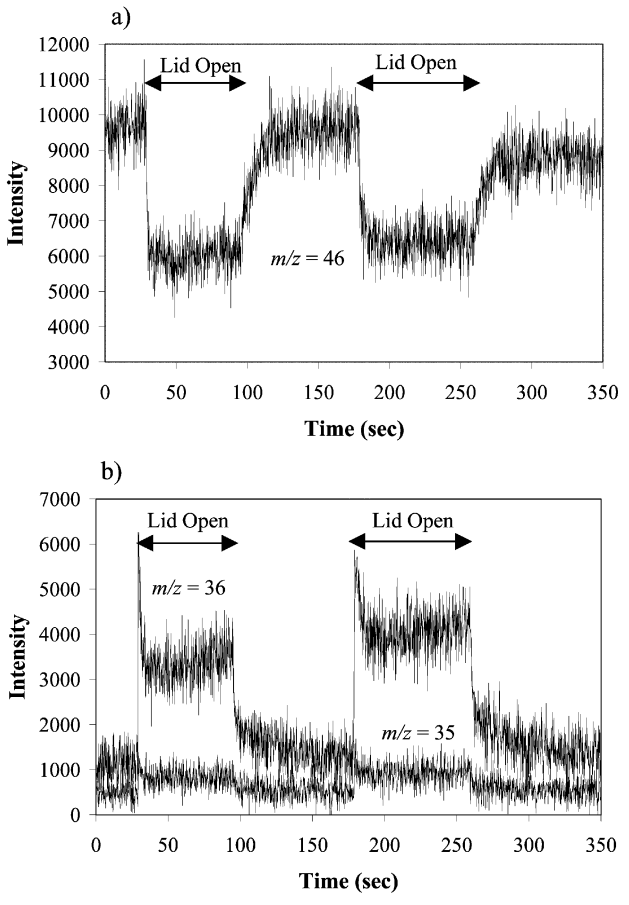

Fig. 2 Uptake of N_2O_5 on 664 particle layers of 10 μm NaCl that had been pumped on for several minutes at room temperature (a) $m/z = 46$ (contributions from N_2O_5, HNO_3 and $ClNO_2$) and (b) $m/z = 35$ and 36 (contributions from HCl and $ClNO_2$). Sample holder surface area was 19.0 cm^2, exit aperture diameter was 3.9 mm, and $[N_2O_5]_0 = 3.5 \times 10^{12}$ molecules cm^{-3} (corrected for a maximum 24% HNO_3 impurity).

Application of correction factors for diffusion into the lower layers of such samples is fraught with significant uncertainties. Therefore, the remaining experiments were conducted using less than one salt layer, and larger particles were used that were visually observed to spread readily and relatively evenly over the sample holder. To determine the portion of a particle layer used in these experiments, the total volume of salt was calculated from the mass of the sample and the density of

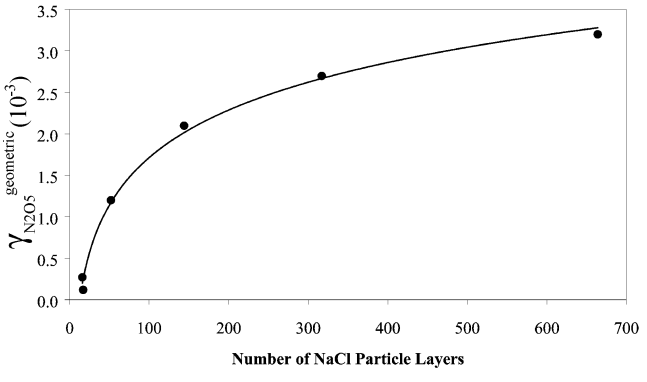

Fig. 3 Uncorrected uptake coefficients for N_2O_5 on NaCl calculated assuming the geometric surface area of the sample holder is the available reactive surface area. The number of layers was calculated as $(m/\rho_b Ah)$, where m is the salt mass, ρ_b is the bulk density determined from the mass of salt required to fill the holder, A is the geometric surface area of the sample holder and h is the height of one salt particle.

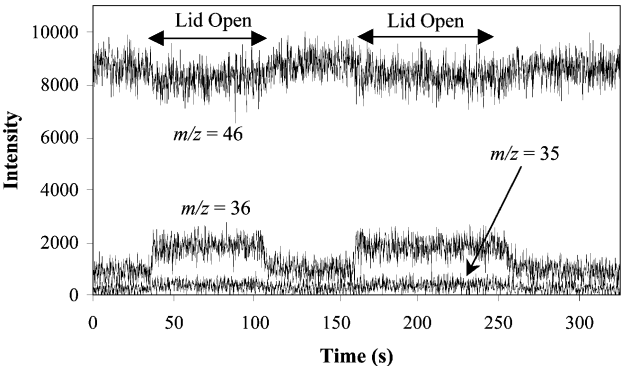

Fig. 4 Uptake of N_2O_5 on a half layer of 312 μm NaCl particles that had been pumped on for several minutes at room temperature. Sample holder surface area was 19.0 cm^2, with an effective surface area of salt particles of 14.5 cm^2, exit aperture diameter was 3.9 mm, and $[N_2O_5]_0 = 4.0 \times 10^{12}$ molecules cm^{-3} (corrected for a maximum 39% HNO_3 impurity).

NaCl, 2.165 g cm^{-3}. The volume per particle was calculated from the average particle size, and the total number of salt particles obtained. Finally, the fraction of the geometric surface of the sample holder covered by the salt particles was calculated from the number of particles and the area of one side of a particle, reported as the fraction of a layer for each experiment.

The results of a typical experiment for N_2O_5 reacting with half a layer of NaCl powder is shown in Fig. 4. The ratio of the $m/z = 36$ to 35 signal is 75% of that for a pure sample of HCl under these conditions, again indicative that $ClNO_2$ is a major product of the N_2O_5 reaction.

B. Model for uptake of gases by a layer or less of salt particles. To obtain the uptake coefficient, the available salt surface area must be known. In order to determine this, the model shown schematically in Fig. 5a was developed. An N_2O_5 molecule can either collide with the top surface of the particles or strike the sample holder between two particles. If it strikes the sample holder, the N_2O_5 molecule can either be scattered away from the sample holder or hit the side of a particle. The available salt surface area thus consists of the tops of the particles and some fraction of the sides. The fraction of molecules that hit the side of a particle can be estimated based on the fraction of open spaces between the particles, the proximity of the adjacent salt particles, and the angle (θ) at which the molecule is scattered. It is assumed that the particles are evenly spaced on the sample holder. Using the cosine law for molecular scattering,[57] the fraction of molecules (F') that scatter at an angle $\geq \theta$, integrated over the 360° horizontal plane, and hit a side of one of the particles after striking the sample holder can be calculated:

$$F' = \cos^2\theta \qquad \text{(VI)}$$

where

$$\theta = 90 - \arctan\frac{a}{b} \qquad \text{(VII)}$$

and a is the height of the salt particle and b is half the distance between two particles (Fig. 5a). This fraction, however, includes open spaces between particles that a molecule may pass through, never striking a particle side. Therefore, to adjust for this, the fraction F' scattered at angles $\geq \theta$ was reduced by calculating the circumference of a circle drawn through the centers of four adjacent particles (Fig. 5b). The fraction of this circumference that was not "covered" by the four particle sides was taken as the opening between the particles. This adjusted fraction is denoted F. (A smaller circle drawn as a tangent to the sides of the particles was found to overcorrect for higher particle coverages, and hence was not

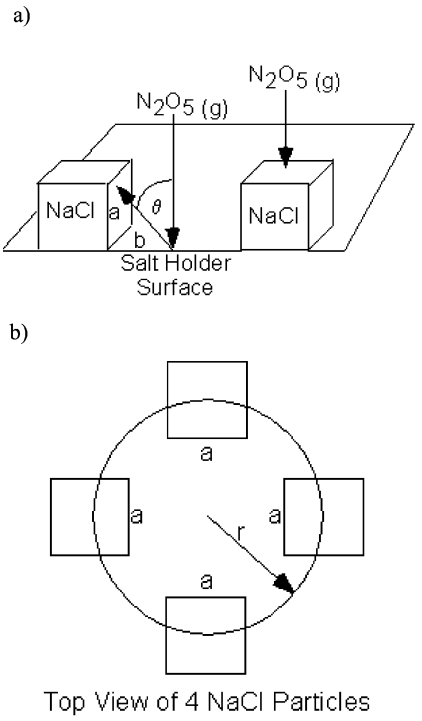

Fig. 5 (a) Diagram of scattering of an N_2O_5 molecule from the sample holder and hitting the side of an NaCl particle. (b) Schematic diagram of method used to correct for spaces between evenly spaced NaCl particles for determination of the available reactive surface.

used.) The true available reactive surface area is then equal to the tops of the particles (A_{tops}) plus the fraction F of the open "holes" between salt particles that the incoming N_2O_5 sees:

$$\text{True reactive area} = A_{tops} + (A_{geometric} - A_{tops})F \quad \text{(VIII)}$$

Using this true reactive surface area, the uptake coefficients for N_2O_5 on fractional layers of NaCl were calculated.

Determining the true available surface area in this manner assumes that N_2O_5 is not taken up irreversibly on the halocarbon wax coating. If it is adsorbed and then subsequently released rather than being scattered directly off the sample holder, this model still applies.[58] The presence of water on the surface is the key to irreversible uptake and reaction of N_2O_5. However, significant amounts of water are not expected under vacuum on the hydrophobic halocarbon wax surface. Supporting this is the fact that there was no measured loss of N_2O_5 when the lid to the sample holder was lifted in the absence of salt.

Table 2 summarizes the uptake coefficients for N_2O_5 on NaCl obtained in this manner, as well as the branching ratios for $ClNO_2$ formation. For comparison, the uptake coefficients measured using the geometrical surface area, $\gamma^{geometric}$, are also listed to provide information on the magnitude of the corrections applied. The corrected uptake coefficients measured using the two particle sizes are consistent, within experimental error, with an overall average value of $(2.9 \pm 1.7) \times 10^{-3}$ (2σ), and an average $ClNO_2$ branching ratio of 0.73 ± 0.28 (2σ). Thus, reaction (2) to generate $ClNO_2$ dominates over the hydrolysis reaction (4). However, the observation of HCl in excess of that calculated to arise from the HNO_3 impurity shows that hydrolysis of N_2O_5 to generate HNO_3, and subsequently HCl, also occurs on these solid salts that hold SAW.

C. Uncertainties in the uptake coefficients. Uncertainties in the calculation of the uptake coefficients are due to potential errors in the following: (1) the random errors in the raw signals; (2) the estimate of the amount of HNO_3 present initially in the N_2O_5 which contributes to the $m/z = 46$ signal both with the lid open and closed; (3) the correction for a contribution of the product $ClNO_2$ to the $m/z = 46$ signal when the lid is open; and (4) the assumptions in the model used to obtain the available surface area.

With respect to the first issue, an error analysis for the data on the experiment shown in Fig. 4 gives an error of 16% (2σ) in the calculated value of the uncorrected (geometric) uptake coefficient. For the second issue, measurements of the HNO_3 impurity using FTIR overestimates the concentration due to hydrolysis of N_2O_5 on the walls of the smaller FTIR cell which was not coated with halocarbon wax (Section II). For the experiment in Fig. 4 in which $\gamma_{N_2O_5}$ was measured to be 3.6×10^{-3}, the uptake coefficient would be calculated to be 2.7×10^{-3} if it is assumed that the HNO_3 impurity is 0% rather than 39%, an error of 25% for this alternate extreme assumption regarding the level of the HNO_3 impurity. With respect to the third issue, the uncertainty associated with the $m/z = 46$ correction for $ClNO_2$ was determined for the same experiment. If the branching ratio for $ClNO_2$ is assumed to

Table 2 Summary of $ClNO_2$ production and uptake coefficient for N_2O_5 on less than one layer of NaCl at 23 °C[a]

Particle size/μm	Mass/g	No. of particle layers	Corrected[d] $[N_2O_5]_0/10^{12}$ molecules cm^{-3}	% HNO_3 impurity[e]	Fraction of HCl from hydrolysis[f]	$\gamma^{geometric}$/units of 10^{-3} [g]	$\gamma_{N_2O_5}$/units of 10^{-3} [h]	BR^{ClNO_2} [i]
312[b]	0.704	0.5	4.0	39	0.74	2.7	3.6	0.75
	0.576	0.4	2.7	39	0.75	1.6	2.4	0.78
	0.390	0.3	3.2	39	0.72	0.9	1.7	0.50
	0.173	0.1	3.2	39	0.50	0.6	2.5	0.60
			Average ($\pm 2\sigma$)[j]:		0.68 ± 0.24		2.6 ± 1.6	0.66 ± 0.26
428[c]	1.099	0.6	5.4	26	0.60	2.7	3.4	0.95
	0.921	0.5	5.6	26	0.79	2.0	2.7	0.75
	0.710	0.4	5.4	26	0.83	2.6	4.2	0.76
			Average ($\pm 2\sigma$)[j]:		0.72 ± 0.22		3.4 ± 1.5	0.82 ± 0.22
			Overall average ($\pm 2\sigma$):[j]		0.70 ± 0.24		2.9 ± 1.7	0.73 ± 0.28

[a] 3.9 mm aperture used. [b] Samples were pumped on for several minutes. [c] Samples were pumped on for more than 2 h. [d] $[N_2O_5]_0$ after correction for HNO_3 impurity. [e] Maximum % HNO_3 impurity in synthesized N_2O_5 mixture determined by FTIR. [f] Calculated as described in text. [g] Calculated as described in text using the geometric surface area of the sample holder. [h] Calculated as described in text using an effective surface area based on the tops of the particles and a fraction of the particle sides. [i] BR^{ClNO_2} = branching ratio for $ClNO_2$, calculated as described in text. [j] $\sigma = \sqrt{\sum_i (x_i - \bar{x})^2/(n-1)}$

be 0% rather than 75% as measured, the uptake coefficient would be 1.9×10^{-3}, an error of 47%. If, on the other extreme, the $ClNO_2$ branching ratio is assumed to be 100%, the uptake coefficient would then be 4.9×10^{-3}, an error of 36%.

Finally, there are potential errors associated with the model assumptions. For example, the particles are assumed to be cubic, but as discussed above, the particles from crushed single crystals are more irregular in shape. In addition, there is a distribution of particle sizes that is not accounted for in our assumption in the calculations that all particles are cubic with sides equal to the average dimension. The particles had average sizes of 312 ± 160 μm and 428 ± 328 μm (2σ), *i.e.* the uncertainty in the particle sizes is in the range of 51%–77%. The particles are also assumed in the model to be evenly distributed over the sample holder. From visual inspection of the samples, this assumption is reasonable.

Using a conservative approach and assuming that these errors are additive, we estimate our uptake coefficient of 2.9×10^{-3} to be within a factor of better than three of the true value.

D. Uptake of N_2O_5 on synthetic sea salt powders. Using the fractional layer approach to study the uptake of N_2O_5 with particles of SSS was problematic because the high water content[26,53] caused significant clumping of the particles that prevented them from spreading relatively evenly over the sample holder as assumed in the model. In addition, the heterogeneous chemical composition of SSS makes it difficult to be confident that the relatively few particles in the small samples are representative of the overall composition of sea salt. Experiments with 1–2 layers of SSS that had not been heated extensively consistently gave an average reaction probability using the geometric surface area of $(3.4 \pm 0.8) \times 10^{-2}$ (2σ); this is an order of magnitude larger than that for comparable numbers of layers of NaCl. In the SSS experiments, the $ClNO_2$ yield was consistently 100%, and the fraction of HCl from hydrolysis was 0%.

E. Application of the model to the $ClONO_2$ reaction with NaCl. Previous studies carried out in this laboratory of reaction (3) for gaseous $ClONO_2$ with less than one layer of NaCl resulted in an uptake coefficient of $\gamma_{ClONO_2} = (6.5 \pm 3.0) \times 10^{-3}$ (2σ).[21] However, this value was based on the assumption that all six sides of the cubic particles were available for reaction. Based on the model in Fig. 5 and Section III.B, this will overestimate the available surface area and hence, underestimate the uptake coefficient. Table 3 summarizes the data from these earlier experiments and the corrected values for the uptake coefficient after application of the model presented here. The average corrected value is $\gamma_{ClONO_2} = (2.4 \pm 1.2) \times 10^{-2}$ (2σ), a factor of three greater than previously reported.[21]

IV. Discussion

A. Uptake coefficient. Our value for the uptake coefficient for N_2O_5 on NaCl, $(2.9 \pm 1.7) \times 10^{-3}$, and the $ClNO_2$ yield are in good agreement with the earlier studies carried out on solid NaCl powders of Livingston and Finlayson-Pitts,[10] and Fenter *et al.*[13] (see Table 1). In addition to the published studies in Table 1, Stewart *et al.*[59] have recently measured the uptake coefficient for N_2O_5 on NaCl aerosols. They report a value of 2×10^{-3} on dry NaCl particles at relative humidities below 50%, in excellent agreement with our results.

In the studies by Fenter *et al.*[13] and Koch *et al.*,[14] the reaction of N_2O_5 with large, smooth surfaces of NaCl, such as windows or those prepared by spray-coating solutions of NaCl in methanol, was significantly slower. This is not surprising since the most reactive sites on the salt surface are expected to be the steps and edges which are prevalent in salt powders. In addition, as discussed in more detail below, water is believed to play an important role in the reaction. NaCl powders have been shown to contain significant amounts of SAW, even after extensive pumping and heating,[17–22] and this strongly adsorbed water is preferentially adsorbed at surface defects, steps, and edges.[24,60–67] Thus, for both of these reasons, finely divided powders are expected to be more reactive than smooth crystalline surfaces.

The uptake coefficient measured in our studies (and in those cited above) is a steady-state value that reflects the available *reactive* surface area; *i.e.* that is not yet covered by $NaNO_3$ generated during the reaction. It is known that in the reactions of NO_2 and HNO_3 with NaCl, SAW acts to mobilize the surface ions during the reaction. This allows the nitrate to recrystallize as it is generated into separate 3-dimensional microcrystallites of $NaNO_3$ attached to the original NaCl particle, exposing fresh NaCl for reaction.[20,22,24,25,27,28,33,68]

It is apparent from our data that the same phenomenon is occurring in these experiments. Thus, in the experiment shown in Fig. 4, the uptake of N_2O_5 continues for more than 3 min without signs of surface saturation. However, from the N_2O_5 concentration in the cell and using $\gamma_{N_2O5} = 2.9 \times 10^{-3}$, the time to react all of the surface chloride is calculated to be only ~10 s, much shorter than is observed in Fig. 4.

The fraction of the surface covered by $NaNO_3$, and hence unavailable for reaction, is not known. While this precludes obtaining the uptake coefficient for N_2O_5 on a *fresh* NaCl surface, the value measured here in steady-state experiments should be applicable to the atmospheric reaction where the same process of surface mobilization-recrystallization likely occurs.

Table 3 Summary of corrected uptake coefficients for $ClONO_2$ on less than one layer of NaCl[a]

Particle size/μm	Mass/g	No. of particle layers[b]	$[ClONO_2]_0/10^{12}$ molecules cm^{-3}	$\gamma^{geometric\ c}$ / units of 10^{-3}	$\gamma_{ClONO_2}{}^{d}$ / units of 10^{-2}
300	0.2107	0.4	0.7	19.0	2.9
400	0.1011	0.2	2.0	7.2	2.5
400	0.0895	0.1	1.3	6.3	2.5
400	0.0594	0.1	1.6	2.4	1.5
Overall average ($\pm 2\sigma$)[e]					2.4 ± 1.2

[a] Data as reported in reference.[21] [b] Calculated as described in text. [c] Uncorrected uptake coefficients for $ClONO_2$ as measured using geometric surface area of sample holder (7.54 cm^2) and an aperture of 5.8 mm. [d] Corrected uptake coefficients calculated as described in text using an effective surface area based on the tops of the particles and a fraction of the particle sides. [e] $\sigma = \sqrt{\sum_i (x_i - \bar{x})^2/(n-1)}$

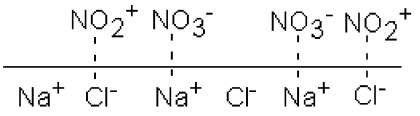

Fig. 6 Electrostatic interaction of ionized N_2O_5 on the surface of NaCl salt particles.

B. Reaction products and branching ratio. Our experiments demonstrate that NaCl powders react with N_2O_5 to generate $ClNO_2$ as the major product, in agreement with the studies summarized in Table 1. However, while $ClNO_2$ is the major product, our observation of HCl in excess of that attributable to the reaction of the HNO_3 impurity in the N_2O_5 (Table 2) suggests that some hydrolysis of N_2O_5 does indeed contribute to its uptake. This is consistent with the known presence of SAW on the particles[17–22] which will lead to hydrolysis of N_2O_5 to form HNO_3/HCl, in competition with $ClNO_2$ formation.

It is important to note that increased amounts of water lead to *increased* $ClNO_2$ production, rather than a decrease as might be expected in the presence of SAW if there was a competition for N_2O_5 between reaction with Cl^- and H_2O. For example, the studies summarized in Table 1 show that aqueous solutions of NaCl generate $ClNO_2$ in essentially 100% yield. In our studies of the reaction with SSS that holds much greater amounts of water than NaCl,[26,53] the $ClNO_2$ yield was 100%, larger than the average of 73% measured for the NaCl reaction. To understand why this is the case, the mechanism must first be described.

The interaction of gaseous N_2O_5 with water on surfaces or in particles is believed to occur *via* autoionization:[1–3,5–9]

$$N_2O_5 \leftrightarrow NO_2^+ + NO_3^- \quad (5)$$

Competition for NO_2^+ then occurs between Cl^- to form $ClNO_2$, and H_2O to form HNO_3. Based on studies of the uptake of N_2O_5 into aqueous solutions of NaCl, Behnke and coworkers[5] reported that the ratio of the rate constants for the reaction of NO_2^+ with Cl^- to that for the reaction with H_2O is 836 ± 32 (1σ). Thus, at a Cl^- concentration of only $\sim$0.07 M, the NO_2^+ ion would be removed at equal rates by reaction with H_2O and Cl^-. The presence of concentrated aqueous phase NaCl solutions should therefore lead to more rapid uptake of N_2O_5 and efficient production of $ClNO_2$, as is the case for SSS. Although SSS has a variety of components[53] that could potentially also participate in the reaction with N_2O_5, the results of previous studies of its reactions with NO_2 and HNO_3[26,53] suggest that the increased water content is the major factor in its increased reactivity compared to NaCl.

In the case of NaCl powders that hold SAW, there is less water available to stabilize the ions formed in the autoionization. On the other hand, as shown in Fig. 6, the surface of NaCl itself may help to stabilize the ion pair through electrostatic interactions. In order to remove chloride ions from the salt matrix and generate gaseous $ClNO_2$, reorganization of the surface of NaCl is required. To accomplish such a reorganization, significant ion mobility is required, and this is known to be enhanced by very small amounts of water on the surface.[17,20,22,24–26,68] However, such surface restructuring and release of $ClNO_2$ aided by SAW will occur in competition with reaction with water on the surface to generate HNO_3. The observation of less than 100% yields of $ClNO_2$ in this and other studies of the reaction of NaCl powders[10,13] suggests that restructuring of the solid surface is occurring at a similar rate to the reaction with HNO_3.

V. Atmospheric implications

As discussed above, the steady-state uptake coefficient measured in these studies is applicable to the reactions of N_2O_5 and $ClONO_2$ in the atmosphere with sea salt particles at relative humidities below the effluorescence point of 45% which occurs as particles are carried inland or to higher altitudes. The generation of photolyzable chlorine compounds such as $ClNO_2$ and Cl_2 occurs in competition with the reaction with HNO_3 to generate HCl. Although the latter can form atomic chlorine *via* the reaction with OH, it is slow relative to deposition of the highly soluble HCl, and hence is unlikely to be a significant source of chlorine atoms in the troposphere. It is therefore important to assess the relative importance of the N_2O_5, $ClONO_2$, and HNO_3 reactions. In addition, the concentrations of $ClNO_2$ and Cl_2 that could be formed overnight, and their contributions to chlorine atom production at dawn, are important.

The relative importance of the reactions of N_2O_5, $ClONO_2$ and HNO_3 will depend on their reaction probabilities as well as the atmospheric concentrations of these species. The reaction probability for HNO_3 under similar experimental conditions has been measured in a separate study[29] to be 6×10^{-4}. Typical concentrations of HNO_3 range from a few ppt in remote regions to $\sim$25 ppb in highly polluted urban areas.[45] The concentration of N_2O_5 has been estimated to be up to $\sim$10 ppb in highly polluted urban atmospheres, based on simultaneous measurements of NO_3 and NO_2 and the known equilibrium constant,[69] and has been measured recently in urban continental air at levels of 100–200 ppt.[70] There are no published measurements of $ClONO_2$ in the troposphere, but model estimates are of the order of 5 ppt.[71,72] Taking levels that might be found in coastal urban areas of 100 ppt for each HNO_3 and N_2O_5, and 5 ppt for $ClONO_2$, the relative rates of reaction of NaCl with N_2O_5 and $ClONO_2$ will be about a factor of five and two greater respectively, than with HNO_3, *i.e.*, $\gamma_{N_2O_5}[N_2O_5] \cong 5\gamma_{HNO_3}[HNO_3]$ and $\gamma_{ClONO_2}[ClONO_2] \cong 2\gamma_{HNO_3}[HNO_3]$.

The amount of $ClNO_2$ that can be formed by this reaction overnight can be estimated from our steady-state reaction probability and the number of collisions per second of N_2O_5 with the salt surface [given by $AG(RT/2\pi M)^{1/2}$, where A is the available surface area, G is the N_2O_5 concentration, and M is the molecular weight of N_2O_5]. A sea salt particle concentration of 5 cm^{-3} with a cubic shape 2 μm on each side was assumed. Using a reaction probability of 2.9×10^{-3} for the N_2O_5 reaction with NaCl, a 73% yield of $ClNO_2$, and an N_2O_5 concentration of 100 ppt, the concentration of $ClNO_2$ generated during 12 h of darkness overnight would be $\sim$65 ppt. However, the reaction on sea salt particles is about an order of magnitude faster than on NaCl and the $ClNO_2$ yield is 100%. Thus, $ClNO_2$ formed in 12 h could be as high as one ppb. Under the same assumptions for the salt particle size and salt concentration, and using $\gamma = 2.4 \times 10^{-2}$ for the $ClONO_2$ reaction, 40 ppt of Cl_2 could be generated overnight. Given the uncertainties involved, this calculation is not radically different from the only reported specific measurement of a peak Cl_2 concentration of 150 ppt[73] and similar measurements of unspecified photolyzable chlorine compounds using a mist chamber technique that are likely mainly Cl_2.[74,75]

Finally, the rate of chlorine atom generation from $ClNO_2$ relative to Cl_2 can be estimated based on their photolysis rate constants calculated from their absorption cross sections, quantum yields and the solar light intensity.[45,76] At a solar zenith angle of 78° (early morning), the photolysis rate constants for $ClNO_2$ and Cl_2 are calculated to be 4.1×10^{-5} and 3.3×10^{-4} s^{-1}, respectively. The rates of production of chlorine atoms under these conditions for 1.0 ppb $ClNO_2$ and 150 ppt Cl_2 are comparable, 1.0×10^6 and 1.2×10^6 atom cm^{-3} s^{-1}, respectively. Given the potential importance of $ClNO_2$ and $ClONO_2$ in coastal urban regions at dawn, it is clearly important to develop specific measurement methods that can be used to search for these species in the marine boundary layer.

Acknowledgements

The authors thank the National Science Foundation (Grant # ATM-0079222) and the Department of Energy (Grant # DE-FG03–98ER62578) for support of this research. We would also like to thank M. A. Kaleuati, M. P. Zach and R. M. Penner for valuable microscopy assistance, J. Greaves for insightful mass spectrometer information, J. C. Hemminger and V. E. Bondybey for helpful discussions and encouragement, and R. A. Cox for permission to cite his work prior to publication. B. S. Fox gratefully acknowledges the Deutsche Forschungsgemeinschaft for travel funding.

References

1 M. Mozurkewich and J. G. Calvert, *J. Geophys. Res.*, 1988, **93**, 15 889.
2 A. Fried, B. E. Henry and J. G. Calvert, *J. Geophys. Res.*, 1994, **99**, 3517.
3 C. George, J. L. Ponche, P. Mirabel, W. Behnke, V. Scheer and C. Zetzsch, *J. Phys. Chem.*, 1994, **98**, 8780.
4 W. B. DeMore, S. P. Sander, D. M. Golden, R. F. Hampson, M. J. Kurylo, C. J. Howard, A. R. Ravishankara, C. E. Kolb and M. J. Molina, *Chemical Kinetics and Photochemical Data for Use in Stratospheric Modeling*, Evaluation No. 12, 1997.
5 W. Behnke, C. George, V. Scheer and C. Zetzsch, *J. Geophys. Res.*, 1997, **102**, 3795.
6 G. N. Robinson, D. R. Worsnop, J. T. Jayne, C. E. Kolb and P. Davidovits, *J. Geophys. Res.*, 1997, **102**, 3583.
7 A. Wahner, T. F. Mentel, M. Sohn and J. Stier, *J. Geophys. Res.*, 1998, **103**, 31 103.
8 F. Schweitzer, P. Mirabel and C. George, *J. Phys. Chem. A*, 1998, **102**, 3942.
9 T. F. Mentel, M. Sohn and A. Wahner, *Phys. Chem. Chem. Phys.*, 1999, **1**, 5451.
10 F. E. Livingston and B. J. Finlayson-Pitts, *Geophys. Res. Lett.*, 1991, **18**, 17.
11 I. M. Msibi, Y. Li, J. P. Schi and R. M. Harrison, *J. Atmos. Chem.*, 1994, **18**, 291.
12 M. T. Leu, R. S. Timonen, L. F. Keyser and Y. L. Yung, *J. Phys. Chem.*, 1995, **99**, 13 203.
13 F. F. Fenter, F. Caloz and M. J. Rossi, *J. Phys. Chem.*, 1996, **100**, 1008.
14 T. G. Koch, H. Van Den Bergh and M. J. Rossi, *Phys. Chem. Chem. Phys.*, 1999, **1**, 2687.
15 W. Behnke, H.-U. Kruger, V. Scheer and C. Zetzsch, *J. Aerosol Sci.*, 1991, **22**, S609.
16 C. Zetzsch and W. Behnke, *Ber. Bunsen-Ges. Phys. Chem.*, 1992, **96**, 488.
17 P. Beichert and B. J. Finlayson-Pitts, *J. Phys. Chem.*, 1996, **100**, 15 218.
18 J. A. Davies and R. A. Cox, *J. Phys. Chem. A*, 1998, **102**, 7631.
19 A. Aguzzi and M. J. Rossi, *Phys. Chem. Chem. Phys.*, 1999, **1**, 433.
20 S. Ghosal and J. C. Hemminger, *J. Phys. Chem. A*, 1999, **103**, 4777.
21 M. E. Gebel and B. J. Finlayson-Pitts, *J. Phys. Chem. A*, 2001, **105**, 5178.
22 S. Ghosal and J. C. Hemminger, *J. Phys. Chem. A*, 2003, submitted.
23 J. M. Laux, J. C. Hemminger and B. J. Finlayson-Pitts, *Geophys. Res. Lett.*, 1994, **21**, 1623.
24 J. M. Laux, T. F. Fister, B. J. Finlayson-Pitts and J. C. Hemminger, *J. Phys. Chem.*, 1996, **100**, 19 891.
25 H. C. Allen, J. M. Laux, R. Vogt, B. J. Finlayson-Pitts and J. C. Hemminger, *J. Phys. Chem.*, 1996, **100**, 6371.
26 D. O. DeHaan and B. J. Finlayson-Pitts, *J. Phys. Chem. A*, 1997, **101**, 9993.
27 C. D. Zangmeister and J. E. Pemberton, *J. Phys. Chem. B*, 1998, **102**, 8950.
28 C. D. Zangmeister and J. E. Pemberton, *J. Phys. Chem. A*, 2001, **105**, 3788.
29 R. C. Hoffman, M. A. Kaleuati and B. J. Finlayson-Pitts, *In preparation*, 2003.
30 W. Behnke and C. Zetzsch, *J. Aerosol Sci.*, 1990, **21**, S229.
31 W. Behnke, V. Scher and C. Zetzsch, *J. Aerosol Sci.*, 1993, **24**, S115.
32 F. F. Fenter, F. Caloz and M. J. Rossi, *J. Phys. Chem.*, 1994, **98**, 9801.
33 D. Sporleder and G. E. Ewing, *J. Phys. Chem. A*, 2001, **105**, 1838.
34 C. Guimbaud, F. Arens, L. Gutzwiller, H. W. Gaggeler and M. Ammann, *Atmos. Chem. Phys. Discuss.*, 2002, **2**, 739.
35 W. C. Keene, A. A. Pszenny, D. J. Jacob, R. A. Duce, J. N. Galloway, J. J. Schultz-Tokos, H. Sievering and J. F. Boatman, *Global Biochem. Cycles*, 1990, **4**, 407.
36 W. L. Chameides, D. D. Davis, J. Bradshaw, S. Sandholm, M. Rodgers, B. Baum, B. Ridley, S. Madronich, M. A. Carroll, G. Gregory, H. I. Schiff, D. R. Hastie, A. Torres and E. Condon, *J. Geophys. Res.*, 1990, **95**, 10 235.
37 W. L. Chameides and A. W. Stelson, *J. Geophys. Res.*, 1992, **97**, 20 565.
38 W. C. Keene, in *Naturally-Produced Organohalogens*, ed. A. Grimvall and E. W. B. d. Leer, Kluwer Academic Publishers, Dordrecht, 1995, pp 363.
39 M. O. Andreae and P. J. Crutzen, *Science*, 1997, **276**, 1052.
40 B. J. Finlayson-Pitts and J. N. J. Pitts, *Science*, 1997, **276**, 1045.
41 A. R. Ravishankara, *Science*, 1997, **276**, 1058.
42 D. O. DeHaan, T. Brauers, K. Oums, J. Stutz, T. Nordmeyer and B. J. Finlayson-Pitts, *Int. Rev. Phys. Chem.*, 1999, **18**, 343.
43 J. C. Hemminger, *Int. Rev. Phys. Chem.*, 1999, **18**, 387.
44 B. J. Finlayson-Pitts and J. C. Hemminger, *J. Phys. Chem. A*, 2000, **104**, 11 463.
45 B. J. Finlayson-Pitts and J. N. J. Pitts, *Chemistry of the Upper and Lower Atmosphere - Theory, Experiments, and Applications*, Academic Press, San Diego, 2000.
46 L. F. Keyser, S. B. Moore and M.-T. Leu, *J. Phys. Chem.*, 1991, **95**, 5496.
47 L. F. Keyser, M.-T. Leu and S. B. Moore, *J. Phys. Chem.*, 1993, **97**, 2800.
48 C. A. Rogaski, D. M. Golden and L. R. Williams, *Geophys. Res. Lett.*, 1997, **24**, 381.
49 A. L. Goodman, G. M. Underwood and V. H. Grassian, *J. Geophys. Res.*, 2000, **105**, 29 053.
50 G. M. Underwood, P. Li, C. R. Usher and V. H. Grassian, *J. Phys. Chem. A*, 2000, **104**, 819.
51 G. M. Underwood, P. Li, H. Al-Abadleh and V. H. Grassian, *J. Phys. Chem. A*, 2001, **105**, 6609.
52 P. Li, H. A. Al-Abadleh and V. H. Grassian, *J. Phys. Chem. A*, 2002, **106**, 1210.
53 S. Langer, R. S. Pemberton and B. J. Finlayson-Pitts, *J. Phys. Chem. A*, 1997, **101**, 1277.
54 I. Wangberg, T. Etzkorn, I. Barnes, U. Platt and K. H. Becker, *J. Phys. Chem. A*, 1997, **101**, 9694.
55 D. M. Golden, G. N. Spokes and S. W. Benson, *Angew. Chem., Int. Ed. Engl.*, 1973, **12**, 534.
56 M. A. Quinlan, C. M. Reihs, D. M. Golden and M. A. Tolbert, *J. Phys. Chem.*, 1990, **94**, 3255.
57 M. D. Boeckmann, *J. Vac. Sci. Technol. A*, 1986, **4**, 353.
58 M. Head-Gordon, J. C. Tully, C. T. Rettner and C. B. Mullins, *J. Chem. Phys.*, 1991, **94**, 1516.
59 D. J. Stewart, J. C. Mossinger, J. W. Adams, A. L. Booth and R. A. Cox, in *27th Annual European Geophyical Society Meeting, April 21–26, 2002, Nice, France*.
60 P. B. Barraclough and P. G. Hall, *Surf. Sci.*, 1974, **46**, 393.
61 R. S. C. Smart and N. Sheppard, *J. Chem. Soc., Faraday Trans. 2*, 1976, **72**, 707.
62 J. Estel, H. Hoinkes, H. Kaarmann, H. Nahr and H. Wilsch, *Surf. Sci.*, 1976, **54**, 393.
63 S. Folsch and M. Henzler, *Surf. Sci.*, 1991, **247**, 269.
64 B. Wassermann, S. Mirbt, J. Reif, J. C. Zink and E. Matthias, *J. Chem. Phys.*, 1993, **98**, 10 049.
65 D. J. Dai and G. E. Ewing, *J. Chem. Phys.*, 1993, **98**, 5050.
66 L. W. Bruch, A. Glebov, J. P. Toennies and H. Weiss, *J. Chem. Phys.*, 1995, **103**, 5109.
67 D. J. Dai, S. J. Peters and G. E. Ewing, *J. Phys. Chem.*, 1995, **99**, 10 299.
68 R. Vogt and B. J. Finlayson-Pitts, *J. Phys. Chem.*, 1994, **98**, 3747.
69 R. Atkinson, A. M. Winer and J. N. Pitts, *Atmos. Environ.*, 1986, **20**, 331.
70 S. S. Brown, H. Stark, S. J. Ciciora and A. R. Ravishankara, *Geophys. Res. Lett.*, 2001, **28**, 3227.
71 R. Sander and P. J. Crutzen, *J. Geophys. Res.*, 1996, **101**, 9121.
72 H. B. Singh and J. F. Kasting, *J. Atmos. Chem.*, 1988, **7**, 261.

73 C. W. Spicer, E. G. Chapman, B. J. Finlayson-Pitts, R. A. Plastridge, J. M. Hubbe, J. M. Fast and C. M. Berkowitz, *Nature*, 1998, **394**, 353.
74 W. C. Keene, J. R. Maben, A. A. Pszenny and J. N. Galloway, *Environ. Sci. Technol.*, 1993, **27**, 866.
75 A. A. Pszenny, W. C. Keene, D. J. Jacob, S. Fan, J. R. Maben, M. P. Zetwo, M. Springer-Young and J. N. Galloway, *Geophys. Res. Lett.*, 2001, **20**, 699.
76 J. A. Ganske, H. N. Berko and B. J. Finlayson-Pitts, *J. Geophys. Res.*, 1992, **97**, 7651.